Ratio Mathematica Volume 47, 2023

Mathematical modelling and application of reduced differential transform method for river pollution

Manan A. Maisuria*
Priti V. Tandel†

Abstract

This paper presents the mathematical model of pollutant transport in a river. To effectively find the analytical solution of the advection-diffusion equation under various forms of suitable initial conditions, the reduced differential transform method (RDTM) is used. Three different initial concentration function cases, including rational, exponential, and power, are analyzed for the present model. A 2D and 3D visual comparison of the solutions obtained for each case is also shown. This article discusses the sufficient condition for convergence of the reduced differential transform approach to solving non-linear differential equations.The convergence results for the concentration functions in each case are briefly described. The present method is highly effective and more efficient in solving real-world problems. For all cases, the amount of phosphate pollutant concentration at various distances and time levels has been examined using numerical and graphical representations. While analyzing actual world problems, the current study demonstrates its effectiveness.

Keywords: Pollutant transport equation; Reduced differential transform method; Convergence; River pollution
2020 AMS subject classifications: 35A22 ,35C10, 35G05 [1]

*Veer Narmad South Gujarat University, Surat, Gujarat, India; mananmaisuria.maths21@vnsgu.ac.in.
†Veer Narmad South Gujarat University, Surat, Gujarat, India; pvtandel@vnsgu.ac.in.
[1]Received on November 17, 2022. Accepted on March 21, 2023. Published online on April 10, 2023. DOI: 10.23755/rm.v41i0.955. ISSN: 1592-7415. eISSN: 2282-8214.

1 Introduction

Accidents involving environmental contamination are common in the process plant, particularly in sectors like the chemical sector, manufacture of agricultural chemicals, natural gas extraction, etc [Li et al., 2009]. Organic materials and heavy metals are frequent and harmful contaminants in water pollution incidents, and examples of organic materials include benzene, naphthalene, phenol, anthracene, alcohol, etc. As a typical hydrocarbon, benzene is poisonous, and cancer-causing [Nomura et al., 2019] It may be inhaled or absorbed via the skin. Because of its low vapor pressure, benzene may be easily spread through the air. Exposure to benzene in the past is a common factor in developing leukemia [Jiang et al., 2018, Tsuji et al., 2018, Meszaros et al., 2017]. In many places, industrial or household human activity-related water contamination is a serious issue [Tchobanoglous et al., 1991]. The contamination of water sources is responsible for the deaths of over 25 million people annually. Models to manage and forecast water quality are vital. When analyzing river water quality, numerous aspects must be addressed, including dissolved oxygen, nitrates, chlorides, phosphates, suspended particles, environmental hormones, and chemical oxygen demand, such as heavy metals and bacteria. Agricultural pollution may degrade surface, and groundwater [Knight et al., 2000].

To satisfy its many needs, society relies heavily on river water, one of the few abundant sources of freshwater [Shi et al., 2019]. To ensure an undisturbed freshwater supply, specific water quality requirements along the rivers must be maintained [Chen et al., 2016]. Agricultural non-point source pollution (ANPSP), caused by the use of agrochemicals in farming, significantly impacts water quality and aquatic ecosystems [Bryan and Kandulu, 2011, Borges et al., 2017]. In 1925, the well-known model of Streeter and Phelps characterized the equilibrium of dissolved oxygen in rivers, marking the beginning of the era of mathematical water quality models. Since then, there have been many updates to this model [Streeter, 1925, James, 1978]. Weighted discretizations and the two-dimensional modified equation method solved the linear, constant coefficient advection-diffusion equation. The modified equivalent equation determines one- and multi-dimensional finite difference method accuracy [Noye and Tan, 1989]. The Eulerian-Lagrangian localized adjoint method (ELLAM) solves the nonlinear Buckley-Leverea equation, which has degenerate diffusion and sharpening near-shock solutions [Dahle et al., 1995]. It is thought that a suitable strategy for identifying and evaluating the production of nutrients produced by management scenarios, which may aid in project prioritization and improve water quality, is extensive modeling of the surface water using tried-and-true techniques. They should be simulated as management scenarios before implementing plans to evaluate their effectiveness

[Fakouri et al., 2019].

Numerous research on the impact of various water management strategies on water quality and quantity have been carried out using multiple models and experimental techniques in diverse places of different sizes with varying objectives. They used a MIKE11 pattern on the Pasikhan River and simulated nitrate and phosphate contaminant concentration. The effects of dumping waste water and draining water into rivers are significant and impact the river's water quality. In addition, Kerich assessed the chemicals used in the Ahero Irrigation Scheme and provided many recommendations to enhance the quality of water retrieved from the drainage canals. For this reason, the most efficient means of purifying water for human consumption in the area were biodegradable chemicals for pest and herbicide management and bio-sand filters [Kerich, 2020]. Groundwater quality in the Blinaja River basin was also investigated by Çadraku using irrigation water quality criteria. According to the findings, the groundwater in the research region is of sufficient quality for irrigating the crops. As well as addressing surface water issues, specific recommendations were made for preserving groundwater quality [Çadraku, 2021]. To solve the advection-dispersion equation (ADE) in rivers backward in time and a one-dimensional domain for different pollution loading patterns, an unique analytical approach was devised using the quasi-reversibility (QR) technique and the Fourier transform tool. To avoid the issue being ill-posed during the inverse solution process, a stability factor is added to the initial transport equation in this approach [Permanoon et al., 2022]. Mass movement is regulated by the molecular diffusion of solutes between mobile and static water in aquifers like the Chalk, which have long diffusion path lengths [Bibby, 1981].

In this paper, we formulate a one-dimensional mathematical model of pollutant transport. The governing equation is a 1D advection-diffusion equation solved by the reduced differential transform method (RDTM). This method requires an initial condition. To generate the initial condition, we have used the concentration of the river Khobistskali for PO_4 pollutant component [Tsuji et al., 2018]. Also, we have discussed the convergence of analytic solutions obtained by RDTM.

Section 2 covers the mathematical formulation of this problem. Section 3 contains the fundamental ideas behind the reduced differential transform method. In section 4, The process for achieving the convergence of the analytic series solution given by RDTM has been discussed. Section 5 includes the numerical outcomes and the convergence of the method for its effectiveness. 2D and 3D plots show a visual representation of the obtained solutions. Section 6 provides a summary of the conclusion.

2 Mathematical Formulation of the problem

Reaction, diffusion, advection, absorption, and sedimentation all have a role in transporting the pollutant material farther downstream. Variables such as the kind of pollution, its physicochemical characteristics, flow characteristics, and the surrounding environment all have a role. Thus, parameters linked to the flow of pollution are prioritized above those relating to the pollutant's nature [Kim and Chapra, 1997].

A linear partial differential equation, the mass transfer equation, is often utilized in research on water, soil, petroleum, the living environment, and several engineering subjects. A linear parabolic partial differential equation, the aforementioned equation is of the first and second orders in terms of time and space, respectively. In the one-dimensional domain (along the river length), the general form of this equation under unstable and non-uniform flow regimes is as follows [Amiri et al., 2021].

$$A\frac{\partial c}{\partial t} = \frac{\partial}{\partial x}\left(AD_x\frac{\partial c}{\partial x}\right) - Av\frac{\partial c}{\partial x} - Akc + Af \tag{1}$$

where c =Pollutant concentration, D_x =Diffusion coefficient along the x-direction, v = Mean flow velocity, k = Coefficient of non-conservation, A = Flow area, f = Source term, x = Distance from starting point of domain, t = Time dimension.

For the entire study, the area of the cross-section of the river is considered a constant. To analyze this problem, we have used the concentration of pollutant substance PO_4 of river Khobistskali. Here Khobistskali river's length is 44800 m. Using past collected data, at time $t = 0$ (any fixed time), the concentration is assumed as a rational, exponential, and power form, and the following values of parameters are used to obtain the solutions. $D_x = 0.55\,\frac{m^2}{sec}$, $v = 0.534930\,\frac{m}{sec}$, $k = 0\,\frac{1}{sec}$ and $f = 0$ [Kachiashvili et al., 2007].

Goodness of fit				
Curve fitting	SSE	R-square	Adjusted R-square	RMSE
Rational	3.89E-06	0.9884	0.9876	0.0003662
Exponential	1.62E-05	0.9515	0.9499	0.0007354
Power	5.55E-06	0.9834	0.9823	0.0004376

Table 1: Statistical indices of initial function

Graphical representations of curve fitting for the initial condition are shown in Figures 1, 2, and 3. Table 1 lists the goodness of fit values for various initial conditions.
Hence this problem is studied for three following different cases:

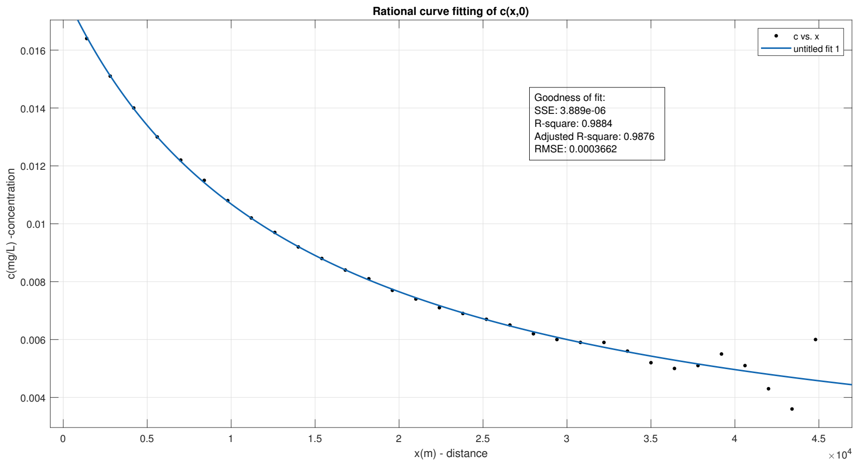

Figure 1: Rational curve fitting of $c(x, 0)$.

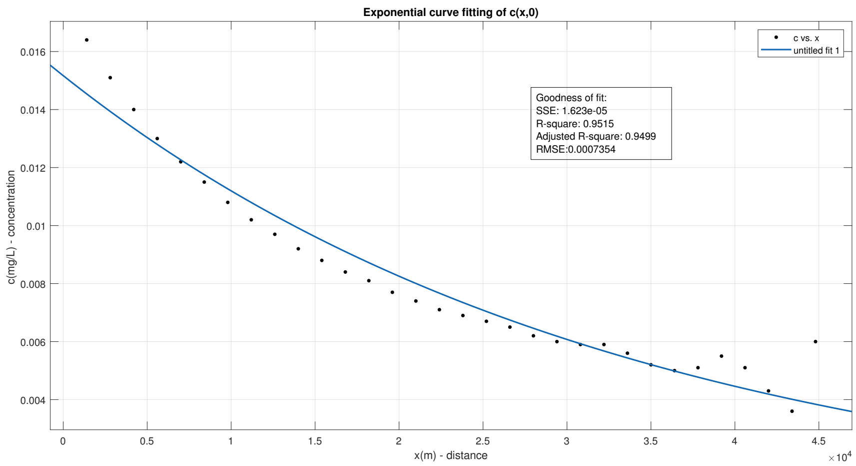

Figure 2: Exponential curve fitting of $c(x, 0)$.

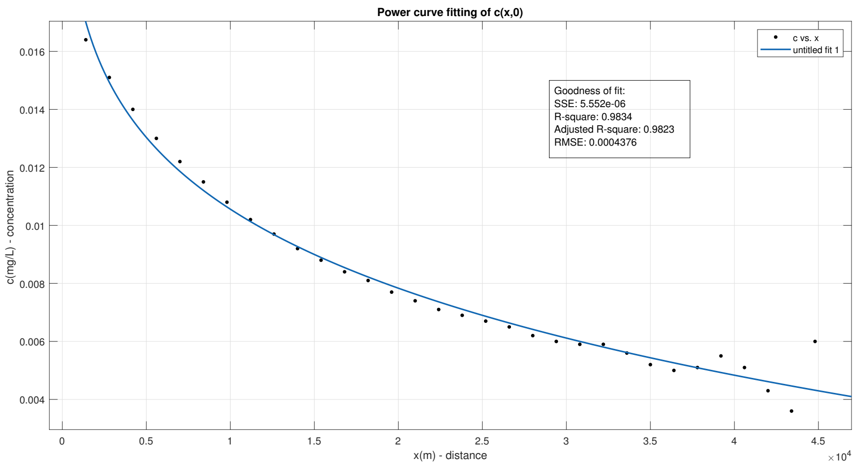

Figure 3: Power curve fitting of $c(x, 0)$.

Case-1 Rational initial function
For this case,

$$c(x,0) = \frac{0.0004008x + 251.4}{x + 1.39e + 04} \tag{2}$$

with

$$c(44800, t) = 5.846e - 13t^2 + 3.463e - 08t + 0.004597 \tag{3}$$

Case-2 Exponential initial function
For this case,

$$c(x,0) = 0.01533e^{-3e-05x} - 0.0001573 \tag{4}$$

with

$$c(44800, t) = 6.887e - 13t^2 + 6.167e - 08t + 0.003846 \tag{5}$$

Case-3 Power initial function
For this case,

$$c(x,0) = -0.007562x^{0.1384} + 0.03762 \tag{6}$$

with

$$c(44800, t) = 6.846e - 08t + 0.004247 \tag{7}$$

3 Reduced Differential Transform Method

Let $b(\omega, \tau)$ be a two-variable function. Suppose $b(\omega, \tau)$ is written as $b(\omega, \tau) = f(\omega)g(\tau).b(\omega, \tau)$ can be represented as the following using the features of the differential transform:

$$b(\omega, \tau) = \sum_{i=0}^{\infty} F_{(i)}\omega^i \sum_{j=0}^{\infty} G_{(j)}\tau^j = \sum_{k=0}^{\infty} B_k(\omega)\tau^k \tag{8}$$

where $B_k(\omega)$ is referred to as the t-dimensional spectrum function of $b(\omega, \tau)$.

$$B_m(\omega) = \frac{1}{m!}\left[\frac{\partial^m}{\partial\tau^m} b(\omega, \tau)\right]_{\tau=0} \tag{9}$$

The original function is denoted by the lowercase $[b(\omega, \tau)]$, whereas the altered function is denoted by the capital $[B(\omega, \tau)]$. The way to define the differential inverse transform of $B_k(\omega)$ is as follows:

$$b(\omega, \tau) = \sum_{m=0}^{\infty} B_m(\omega)\tau^m \tag{10}$$

From Equations (9) and (10), we get

$$b(\omega, \tau) = \sum_{m=0}^{\infty} \frac{1}{m!}\left[\frac{\partial^m}{\partial\tau^m} b(\omega, \tau)\right]_{\tau=0} \tau^m \tag{11}$$

Let us consider the following nonlinear PDE, to understand the basic concept of RDTM.

$$Tb(\omega, \tau) + Pb(\omega, \tau) + Ob(\omega, \tau) = f(\omega, \tau) \tag{12}$$

with initial condition $b(\omega, 0) = \eta(\omega)$
, where $T = \frac{\partial}{\partial\tau}$, $Pb(\omega, \tau)$ is a linear term that has partial derivatives, while $Ob(\omega, \tau)$ is a non-linear term, and $f(\omega, \tau)$ is a source term [Al-Amr, 2014].
By applying the transform on equation (12), we get

$$(m + 1)B_{m+1}(\omega) = F_m(\omega) - PB_m(\omega) - OB_m(\omega) \tag{13}$$

where $B_m(\omega)$,$F_m(\omega)$,$PB_m(\omega)$ and $OB_m(\omega)$ are transform of $b(\omega, \tau)$,$f(\omega, \tau)$,$Pb(\omega, \tau)$

and $Ob(\omega,\tau)$ respectively. We are able to write this down based on the initial condition.

$$B_0(\omega)=\eta(\omega) \tag{14}$$

From equations (13) and (14), we get the values of $B_m(\omega)$. After that, an approximation solution is produced by carrying out an inverse transformation on the set of values $\{B_m(\omega)\}_{m=0}^{n}$. This transformation yields an approximation solution as

$$\tilde{b}_n(\omega,\tau)=\sum_{m=0}^{n}B_m(\omega)\tau^m \tag{15}$$

where n is the order of approximation answer. Consequently, the exact solution is given by [Al-Amr, 2014],

$$b(\omega,\tau)=\lim_{n\to\infty}\tilde{b}_n(\omega,\tau) \tag{16}$$

Function	Transformation
$b(\omega,\tau)$	$B_m(\omega)=\frac{1}{m!}\left[\frac{\partial^m}{\partial\tau^m}b(\omega,\tau)\right]_{\tau=0}$
$\alpha f(\omega,\tau)\pm\beta g(\omega,\tau)$	$\alpha F_m(\omega)+\beta G_m(\omega)$
$\omega^k\tau^n$	$\omega^k\delta(m-n)$
$\omega^k\tau^n b(\omega,\tau)$	$\omega^k B_{m-n}(\omega)$
$l(\omega,\tau)=f(\omega,\tau)g(\omega,\tau)$	$L_m(\omega)=\sum_{r=0}^{m}F_r(\omega)G_{m-r}(\omega)$
$\frac{\partial^r}{\partial\tau^r}b(\omega,\tau)$	$\frac{(m+r)!}{m!}B_{m+r}(\omega)$
$\frac{\partial}{\partial\omega}b(\omega,\tau)$	$\frac{\partial}{\partial\omega}B_m(\omega)$

Table 2: Transform Table[Al-Amr, 2014, Keskin and Oturanc, 2010, Srivastava et al., 2014]

4 Convergence of RDTM

To understand the convergence, Let us consider the solution of equation (13) in power series form as follow

$$b(\omega,\tau)=\sum_{n=0}^{\infty}B_n(\omega)\tau^n=\sum_{n=0}^{\infty}B_n\tau^n \tag{17}$$

which is obtained by equation (16) [Moosavi Noori and Taghizadeh, 2021, Saeed and Mustafa, 2017].

Theorem 4.1. *If* $\sum_{n=0}^{\infty} B_n \tau^n$ *is given series,*

[1] $\exists\, 0 < \beta < 1 \ni \frac{\|B_{n+1}\|}{\|B_n\|} \leq \beta \Rightarrow$ *series is convergent.*

[2] $\exists\, \beta > 1 \ni \frac{\|B_{n+1}\|}{\|B_n\|} \geq \beta \Rightarrow$ *series is divergent.*

Proof. Let $(C[l], \|.\|)$ represent the Banach space that contains all continuous functions on l that satisfy the norm $\|.\|$. Also, let's suppose that $\|B_0(\omega)\| \leq M$, where M is an integer in the positive range. Let $\{\delta_n\}_{n=0}^{\infty}$ be a partial sum

$$\delta_n = B_0 + B_1 + B_2 + ... + B_n$$

If we can prove that $\{\delta_n\}_{n=0}^{\infty}$ is a Cauchy sequence in Banach Space, then we can conclude that the sequence of partial sum is convergent in Banach Space. As a result, at this point, we shall demonstrate that the series of partial sums follows the Cauchy sequence. We take

$$\|\delta_{n+1} - \delta_n\| = \|B_{n+1}\| \leq \beta\|B_n\| \leq ... \leq \beta^{n+1}\|B_0\| \leq \beta^{n+1}M$$

Therefore,$\forall n, m \in \mathbb{N}, n \geq m$,We have

$$\begin{aligned} \|\delta_n - \delta_m\| &= \|(\delta_n - \delta_{n-1}) + (\delta_{n-1} - \delta_{n-2}) + ... + (\delta_{m+1} - \delta_m)\| \\ &\leq \|\delta_n - \delta_{n-1}\| + \|\delta_{n-1} - \delta_{n-2}\| + ... + \|\delta_{m+1} - \delta_m\| \\ &\leq \frac{1-\beta^{n-m}}{1-\beta}\beta^{m+1}\|B_0\| \end{aligned}$$

Now here $0 < \beta < 1$, We obtain

$$\lim_{n,m\to\infty} \|\delta_n - \delta_m\| = 0$$

Hence $\{\delta_n\}_{n=0}^{\infty}$ is Cauchy sequence in Banach Space. Therefore, given series is convergent.

5 Result and discussion

We take three cases of initial function in rational, exponential and power form and obtain three solutions using reduced differential transform method.

Case-1 Rational initial function

Solving equation (1) by RDTM with initial condition (2), we get

$$c(x,t) = M_0 + M_1 t + M_2 t^2 + M_3 t^3 + M_4 t^4 + ...$$

where

$$M_0 = \frac{0.0004008x+251.4}{x+1.39e+04}$$

$$M_1 = \frac{0.0270\left(4863\,x + 67605700\right)}{(x+13900)^3}$$

$$M_2 = \frac{8.9236e{-}06\begin{pmatrix} x^2 + 219193889400\,x \\ +1523735609830000 \end{pmatrix}}{(x+13900)^5}$$

$$M_3 = \frac{9.8159e{-}10\begin{pmatrix} x^3 + 1599028070073300\,x^2 \\ +22233066963300870000\,x \\ +103043693991250631000000 \end{pmatrix}}{(x+13900)^7}$$

$$M_4 = \frac{1.0798e{-}13\begin{pmatrix} 186421425071787\,x^4 \\ +10368864699446257200\,x^3 \\ +216270792211342627620000\,x^2 \\ +2004850662624966111612000000\,x \\ +6969433288195869001126700000000 \end{pmatrix}}{(x+13900)^9}$$

Here,

$$\frac{\|M_1\|}{\|M_0\|} = 3.4116405e-05 < 1, \frac{\|M_2\|}{\|M_1\|} = 3.4972143e-05 < 1,$$

$$\frac{\|M_3\|}{\|M_2\|} = 3.4976844e-05 < 1, \frac{\|M_4\|}{\|M_3\|} = 3.4981545e-05 < 1$$

Therefore, the solution function $c(x,t)$ is convergent.

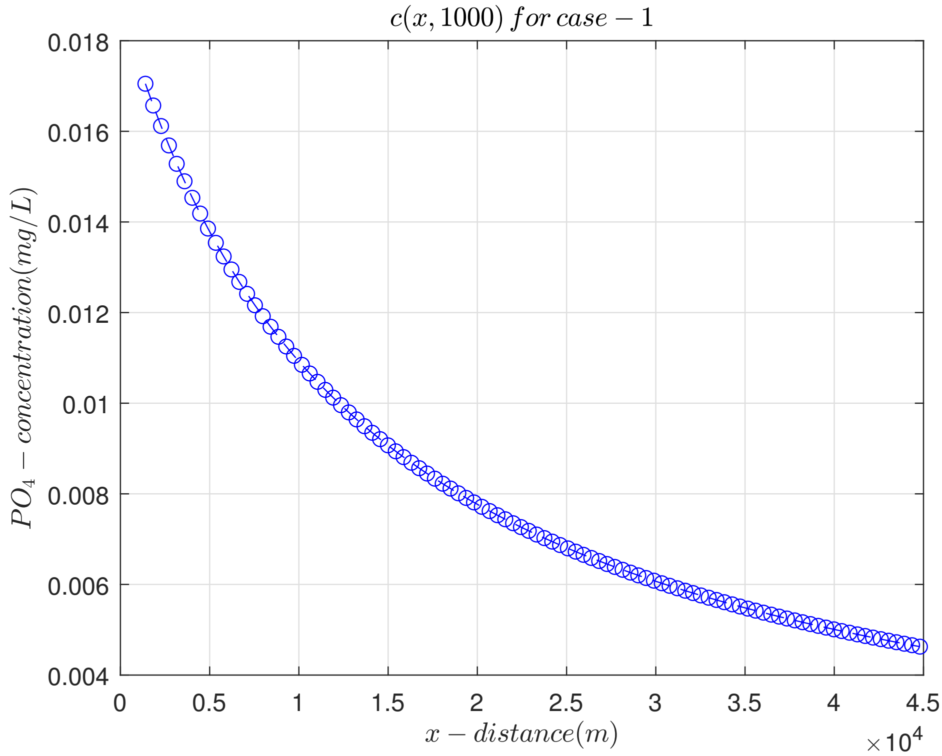

Figure 4: $c(x,t)$ at $t = 1000\,sec$

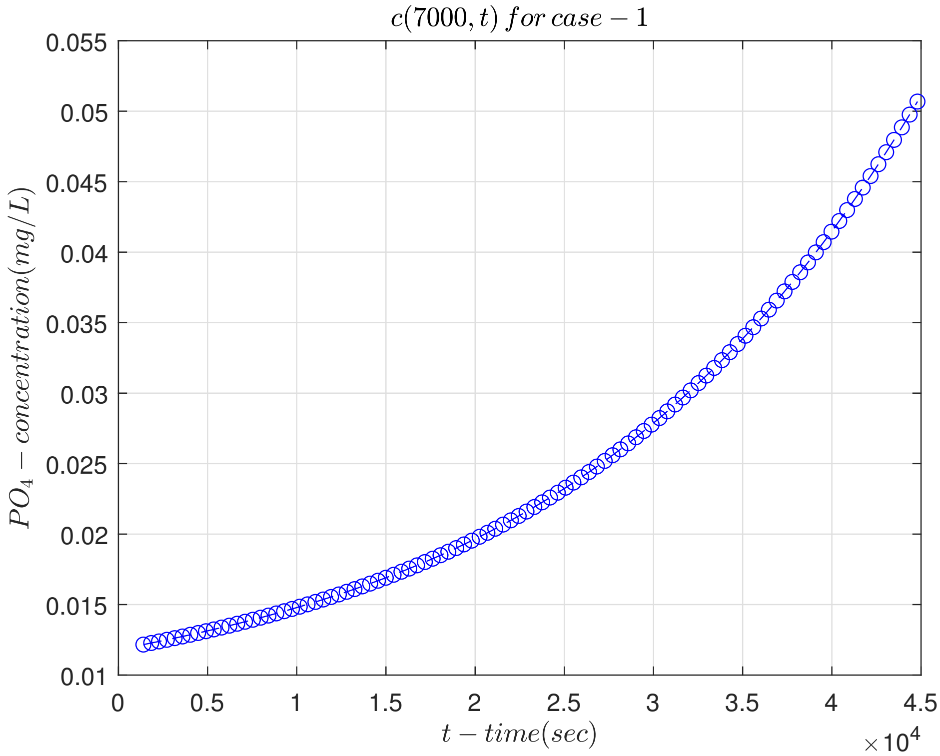

Figure 5: $c(x, t)$ at $x = 7000\, m$

Two-dimensional representations of the concentration function for case-1 are provided in figures 4, and 5, respectively, for the fixed values of ($t = 1000sec$),and ($x = 7000m$).As shown in figure 4, we can see that the value of concentration decreases as the length (x) variable increases. In figure 5, we can see that the value of concentration rises as the passage of time (t) increases.

x(m)\t(sec)	4500	9000	13500	18000	22500	27000	31500	36000
1400	0.019467	0.023775	0.030123	0.039479	0.053046	0.072264	0.098812	0.134601
5740	0.014666	0.016968	0.020065	0.024264	0.029941	0.03754	0.047573	0.060618
10080	0.011796	0.013224	0.015034	0.017353	0.020329	0.024138	0.028979	0.035078
14420	0.009888	0.010858	0.01204	0.013494	0.015289	0.017506	0.020238	0.023587
18760	0.008527	0.009229	0.01006	0.011051	0.01224	0.013668	0.015383	0.017437
23100	0.007507	0.008038	0.008654	0.009372	0.010213	0.011201	0.012363	0.013728
27440	0.006715	0.007131	0.007605	0.008148	0.008772	0.009493	0.010326	0.01129
31780	0.006082	0.006416	0.006792	0.007217	0.007698	0.008246	0.00887	0.009581
36120	0.005564	0.005839	0.006144	0.006485	0.006868	0.007297	0.00778	0.008325
40460	0.005133	0.005362	0.005616	0.005896	0.006206	0.006551	0.006936	0.007365
44800	0.004768	0.004963	0.005176	0.00541	0.005667	0.00595	0.006264	0.00661

Table 3: $c(x,t)$ for Case-1

The values of the concentration function for case-1 are shown in table 3.

Case-2 Exponential initial function

Solving equation (1) by RDTM with initial condition (4), we get

$$c(x,t) = A_0 + A_1 t + A_2 t^2 + A_3 t^3 + A_4 t^4 + ...$$

where

$$\begin{aligned}
A_0 &= 0.01533e^{-3e-05x} - 0.0001573 \\
A_1 &= 2.4602e - 07\,\mathrm{e}^{-\frac{3\,x}{100000}} \\
A_2 &= 1.9741e - 12\,\mathrm{e}^{-\frac{3\,x}{100000}} \\
A_3 &= 1.0561e - 17\,\mathrm{e}^{-\frac{3\,x}{100000}} \\
A_4 &= 4.2370e - 23\,\mathrm{e}^{-\frac{3\,x}{100000}}
\end{aligned}$$

Here,

$$\frac{\|A_1\|}{\|A_0\|} = 1.6221987e - 05 < 1, \frac{\|A_2\|}{\|A_1\|} = 8.0241975e - 06 < 1,$$

$$\frac{\|A_3\|}{\|A_2\|} = 5.3494650e - 06 < 1, \frac{\|A_4\|}{\|A_3\|} = 4.0120987e - 06 < 1$$

Therefore, the solution function $c(x, t)$ is convergent. Figures 6 and 7 illustrate,

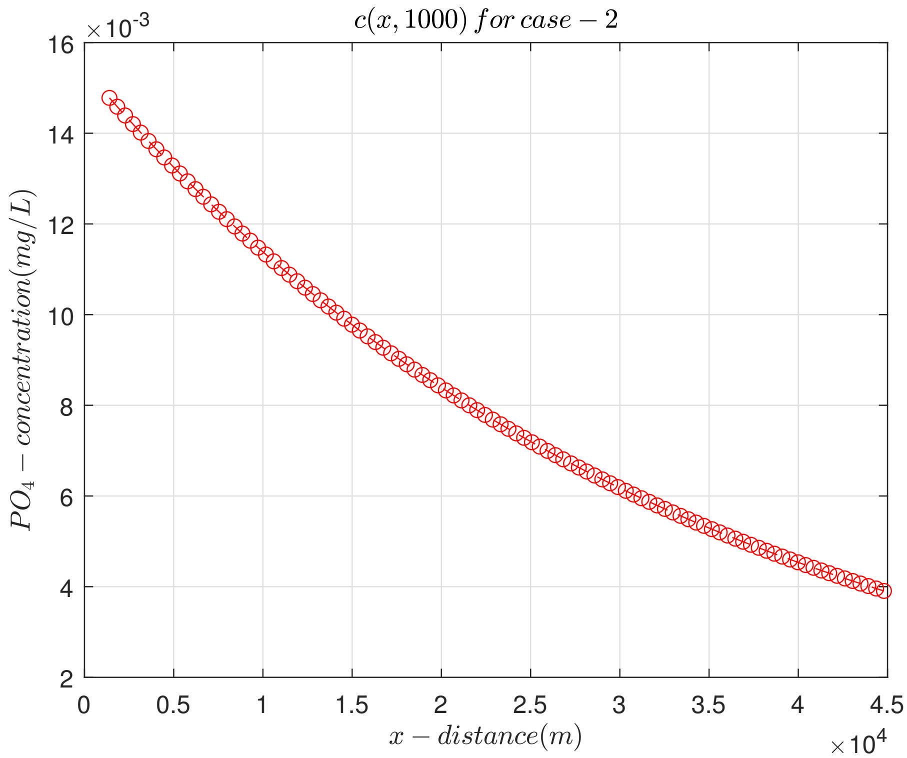

Figure 6: $c(x, t)$ at $t = 1000\, sec$

respectively, two-dimensional representations of the concentration function for case-2 with the fixed values of ($t = 1000\, sec$) and ($x = 7000\, m$). As shown in figure 6, the concentration value falls as the distance (x) variable rises. It is clear from graph 7 that when time (t) grows, so does the value of concentration.

The values of a concentration function for case-2 are presented in table 4.

Case-3 Power initial function

Solving equation (1) by RDTM with initial condition (6), we get

$$c(x, t) = P_0 + P_1 t + P_2 t^2 + P_3 t^3 + P_4 t^4 + ...$$

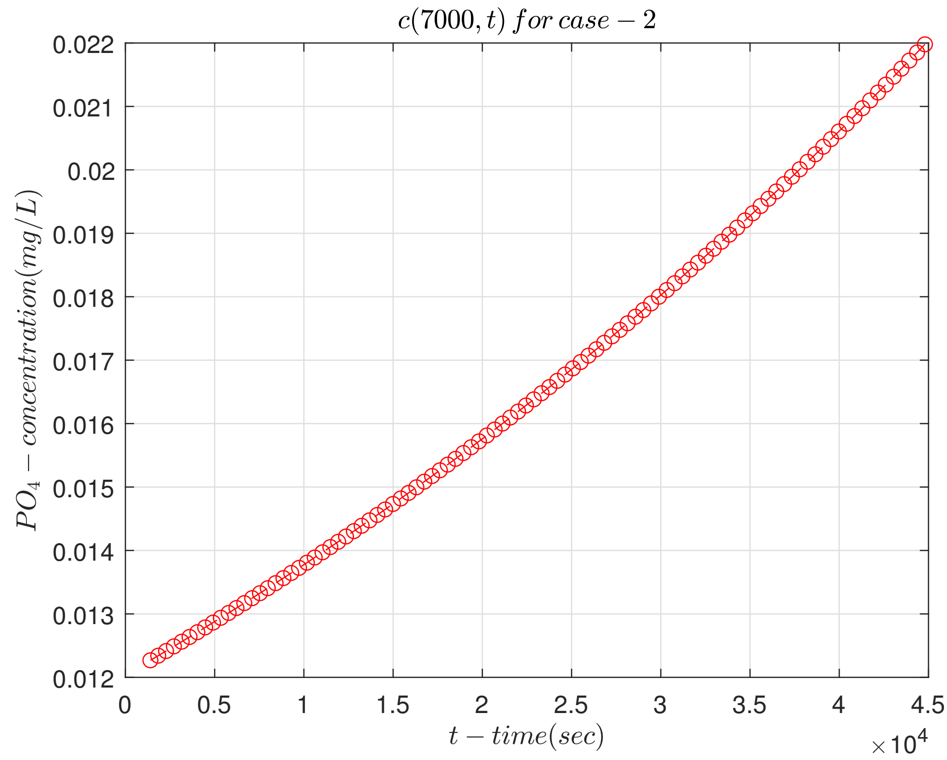

Figure 7: $c(x, t)$ at $x = 7000\,m$

x(m)\t(sec)	4500	9000	13500	18000	22500	27000	31500	36000
1400	0.015643	0.016826	0.018098	0.019465	0.020934	0.022512	0.024208	0.026029
5740	0.013714	0.014753	0.015869	0.01707	0.018359	0.019745	0.021233	0.022832
10080	0.012021	0.012933	0.013913	0.014966	0.016099	0.017315	0.018622	0.020025
14420	0.010534	0.011335	0.012195	0.01312	0.014114	0.015182	0.016329	0.017561
18760	0.009229	0.009932	0.010687	0.011499	0.012372	0.01331	0.014317	0.015398
23100	0.008083	0.0087	0.009363	0.010076	0.010842	0.011665	0.01255	0.013499
27440	0.007077	0.007619	0.008201	0.008827	0.0095	0.010222	0.010998	0.011832
31780	0.006194	0.006669	0.007181	0.00773	0.008321	0.008955	0.009637	0.010368
36120	0.005418	0.005836	0.006285	0.006767	0.007286	0.007843	0.008441	0.009083
40460	0.004738	0.005104	0.005498	0.005922	0.006377	0.006866	0.007391	0.007955
44800	0.00414	0.004462	0.004808	0.00518	0.005579	0.006009	0.00647	0.006965

Table 4: $c(x, t)$ for Case-2

where

$$P_0 = -0.007562x^{0.1384} + 0.03762$$

$$P_1 = \frac{3.4537e{-}07\,(1621\,x+1436)}{x^{2327/1250}}$$

$$P_2 = \frac{1.2902e{-}04\,x^2+4.9388e{-}04\,x+7.2656e{-}04}{x^{4827/1250}}$$

$$P_3 = \frac{4.2826e{-}05\,x^3+3.7801e{-}04\,x^2+0.0015\,x+0.0025}{x^{7327/1250}}$$

$$P_4 = \frac{1.6389e{-}05\,x^4+2.6028e{-}04\,x^3+0.0020\,x^2+0.0078\,x+0.0138}{x^{9827/1250}}$$

Here,

$$\frac{\|P_1\|}{\|P_0\|} = 6.4108463e - 05 < 1, \frac{\|P_2\|}{\|P_1\|} = 0.0001649 < 1,$$

$$\frac{\|P_3\|}{\|P_2\|} = 0.0002379 < 1, \frac{\|P_4\|}{\|P_3\|} = 0.0002747 < 1$$

Therefore, the solution function $c(x,t)$ is convergent. Figures 8 and 9 are two-dimensional representations of the concentration function for case-3 with fixed parameters ($t = 1000sec$) and ($x = 7000m$), respectively. As shown in figure 8, as the distance (x) variable increases, the concentration value decreases. Graph 9 demonstrates that as time (t) increases, so does the value of concentration. The values of a concentration function for case-3 are shown in table 5.

x(m)\t(sec)	4500	9000	13500	18000	22500	27000	31500	36000
1400	0.034284	0.149754	0.560422	1.579016	3.633997	7.269557	13.14562	22.03783
5740	0.014373	0.017404	0.02281	0.032238	0.047824	0.072202	0.108497	0.160329
10080	0.011539	0.012841	0.014609	0.017063	0.020482	0.025201	0.031609	0.040152
14420	0.00987	0.010713	0.011738	0.013011	0.014609	0.016626	0.019168	0.022356
18760	0.00866	0.009291	0.010017	0.010867	0.011871	0.013066	0.014494	0.016203
23100	0.007701	0.008209	0.008775	0.009415	0.010143	0.010977	0.011937	0.013046
27440	0.006902	0.007329	0.007796	0.008311	0.008883	0.009521	0.010237	0.011043
31780	0.006215	0.006584	0.006983	0.007416	0.007888	0.008405	0.008974	0.009603
36120	0.00561	0.005937	0.006285	0.006659	0.007062	0.007498	0.007971	0.008486
40460	0.005069	0.005362	0.005673	0.006003	0.006355	0.006732	0.007137	0.007573
44800	0.004579	0.004845	0.005126	0.005422	0.005735	0.006068	0.006423	0.006801

Table 5: $c(x,t)$ for Case-3

Figure 10 give the 3D graphical comparison of solution obtained for all cases. Also figures 11 and 12 give the 2D graphical comparison of solution obtained for all cases for $t = 3000\,sec$ and $x = 40000\,m$ respectively.

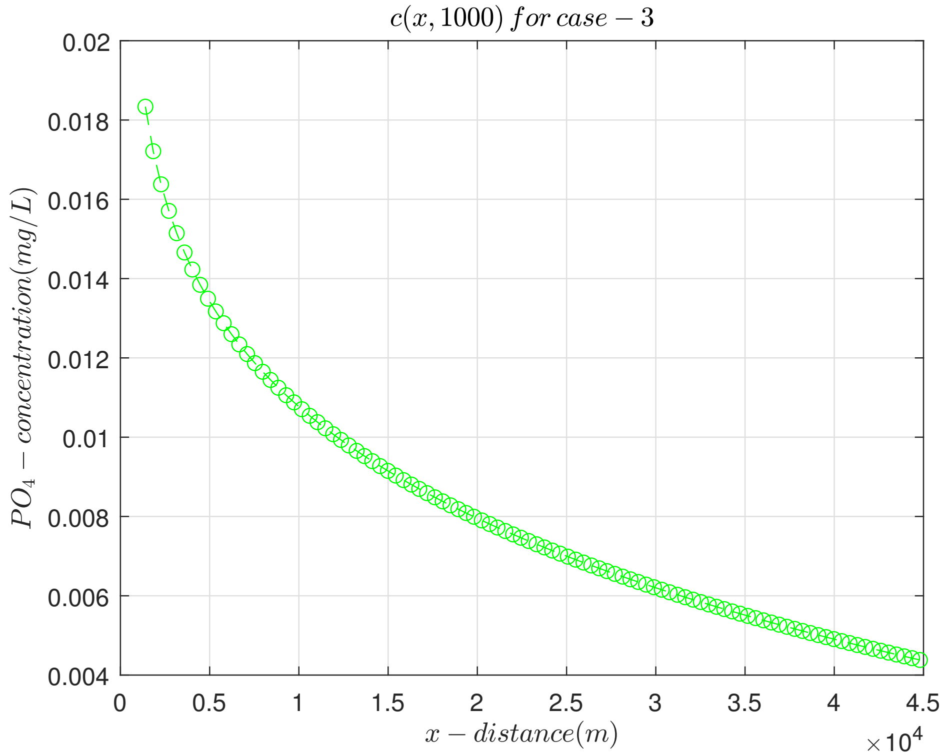

Figure 8: $c(x,t)$ at $t = 1000\,sec$

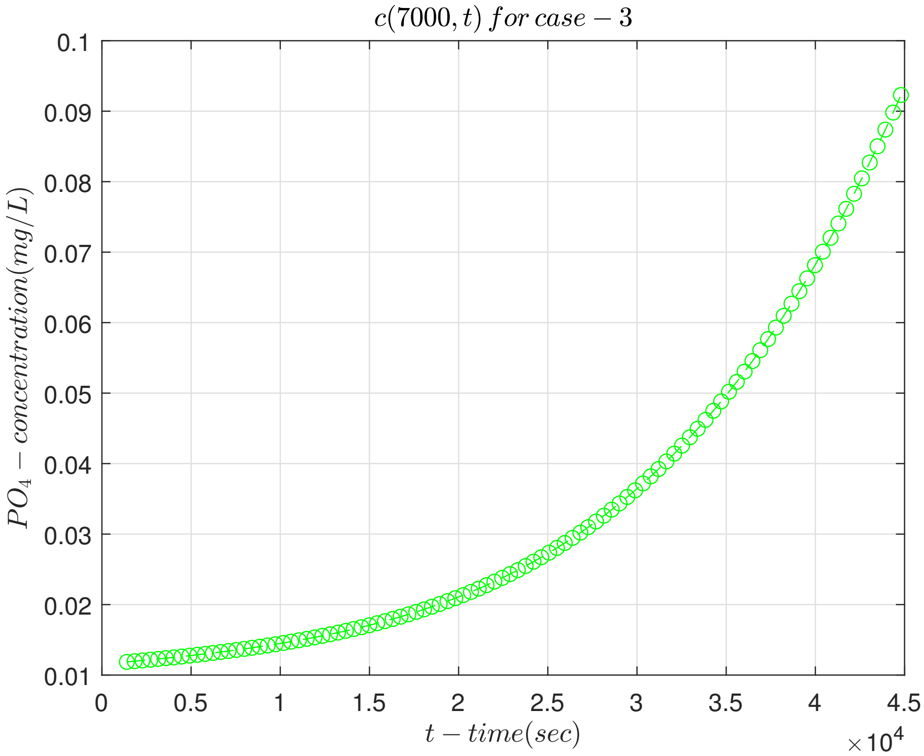

Figure 9: $c(x, t)$ at $x = 7000\, m$

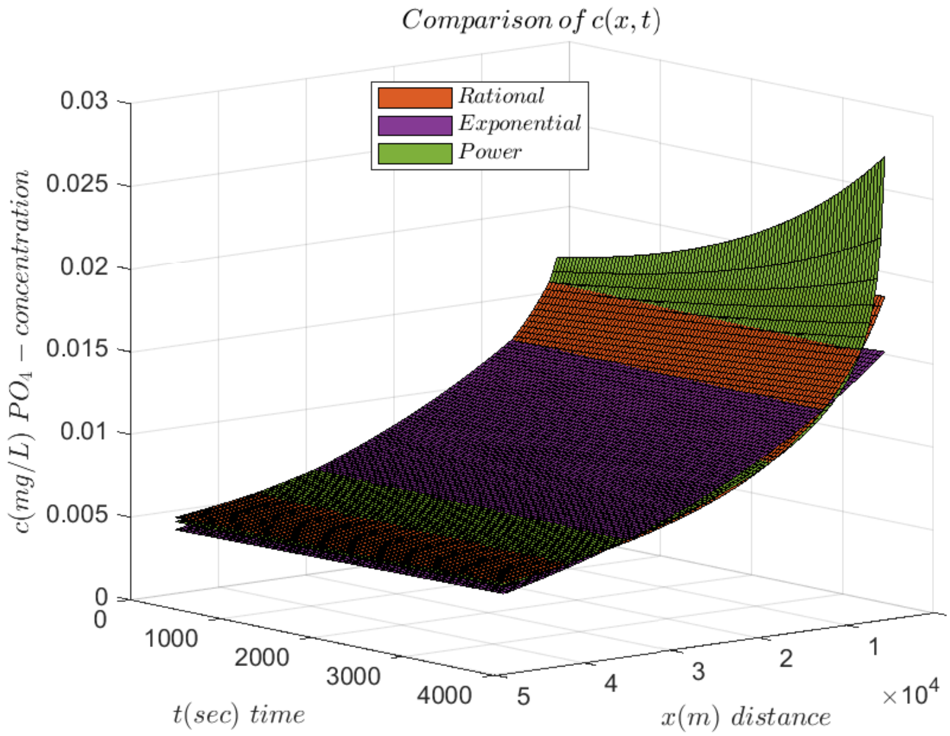

Figure 10: 3D Comparison of $c(x, t)$

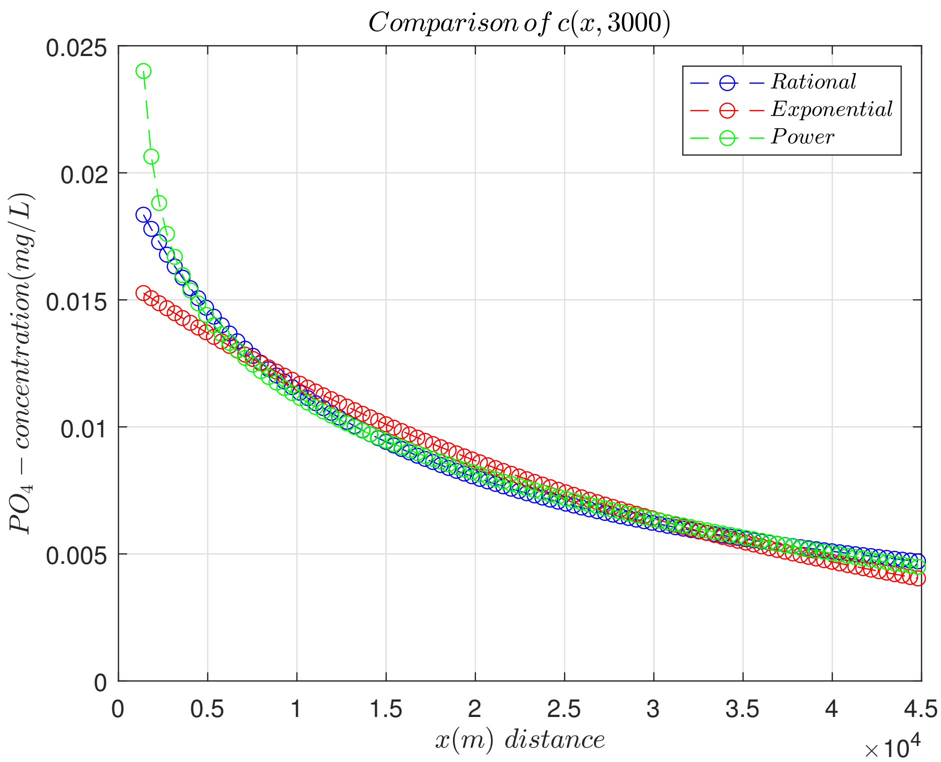

Figure 11: 2D Comparison of $c(x, 3000)$

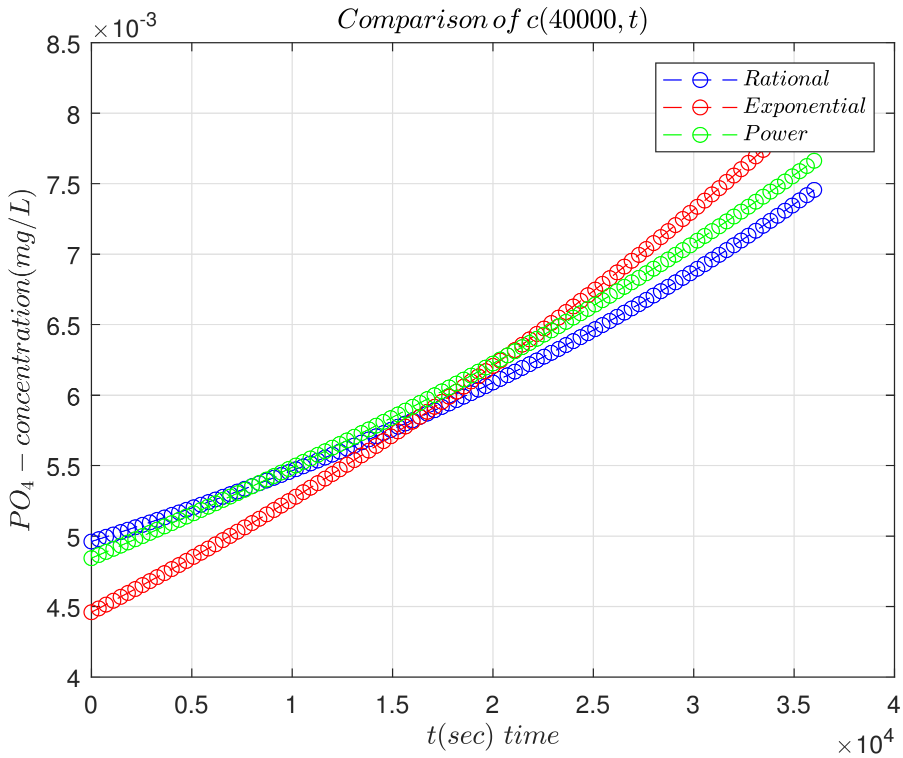

Figure 12: 2D Comparison of $c(40000, t)$

6 Conclusion

In this paper, we outlined the main components of a mathematical model that various ways to predict chemical concentrations in rivers due to pollutant discharges. We get initial condition from old collected data in different form like rational, exponential and power. We attain three different solutions from different form of initial conditions. We conclude that concentration rises as time(t) rises. Concentration decreases as length(x) increases. The fundamental benefit of the RDTM is that it offers the user a quick converging power series form with neatly calculated terms that contains an analytical approximation, and in many situations, an exact solution. There is no discretization or unavoidable presumptions while using RDTM. Sometimes RDTM is superior to other techniques (DTM). Furthermore, if highly polluted regions can be located physically, the research framework may provide a useful strategy for more economical watershed management.According to the findings, phosphate levels along the river fall when fertiliser usage is reduced. Among the management options, the use of less fertiliser greatly reduces river pollution. The current work provides a helpful tool for a scholar to compare and contrast the performance of different models and yields intriguing and practical outcomes. It may be possible to extend this research to consider the two-dimensional advection-diffusion equation.

References

M. O. Al-Amr. New applications of reduced differential transform method. *Alexandria Engineering Journal*, 53(1):243–247, 2014. doi: 10.1016/j.aej.2014.01.003.

S. Amiri, M. Mazaheri, and N. Bavandpouri Gilan. Introducing a new method for calculating the spatial and temporal distribution of pollutants in rivers. *International Journal of Environmental Science and Technology*, 18(12):3777–3794, 2021. doi: 10.1007/s13762-020-03096-y.

R. Bibby. Mass transport of solutes in dual-porosity media. *Water Resources Research*, 17(4):1075–1081, 1981. doi: 10.1029/WR017i004p01075.

L. G. A. Borges, A. Savi, C. Teixeira, R. P. de Oliveira, M. L. F. De Camillis, R. Wickert, S. F. M. Brodt, T. F. Tonietto, R. Cremonese, L. S. da Silva, et al. Mechanical ventilation weaning protocol improves medical adherence and results. *Journal of critical care*, 41:296–302, 2017. doi: 10.1016/j.jcrc.2017.07.014.

B. A. Bryan and J. M. Kandulu. Designing a policy mix and sequence for mitigating agricultural non-point source pollution in a water supply catchment. *Water resources management*, 25(3):875–892, 2011. doi: 10.1007/s11269-010-9731-8.

H. S. Çadraku. Groundwater quality assessment for irrigation: case study in the blinaja river basin, kosovo. *Civil Engineering Journal*, 7(9):1515–1528, 2021.

J. Chen, H. Shi, B. Sivakumar, and M. R. Peart. Population, water, food, energy and dams. *Renewable and Sustainable Energy Reviews*, 56:18–28, 2016. doi: 10.1016/j.rser.2015.11.043.

H. K. Dahle, R. E. Ewing, and T. F. Russell. Eulerian-lagrangian localized adjoint methods for a nonlinear advection-diffusion equation. *Computer methods in applied mechanics and engineering*, 122(3-4):223–250, 1995. doi: 10.1016/0045-7825(94)00733-4.

B. Fakouri, M. Mazaheri, and J. M. Samani. Management scenarios methodology for salinity control in rivers (case study: Karoon river, iran). *Journal of Water Supply: Research and Technology-Aqua*, 68(1):74–86, 2019. doi: 10.2166/aqua.2018.056.

A. James. *Mathematical models in water pollution control*. Wiley, 1978.

B. Jiang, Y. Wen, Z. Li, D. Xia, and X. Liu. Theoretical analysis on the removal of cyclic volatile organic compounds by non-thermal plasma. *Water, Air, & Soil Pollution*, 229(2):1–12, 2018. doi: 10.1007/s11270-018-3687-3.

K. Kachiashvili, D. Gordeziani, R. Lazarov, and D. Melikdzhanian. Modeling and simulation of pollutants transport in rivers. *Applied mathematical modelling*, 31 (7):1371–1396, 2007. doi: 10.1016/j.apm.2006.02.015.

E. C. Kerich. Households drinking water sources and treatment methods options in a regional irrigation scheme. *Journal of Human, Earth, and Future*, 1(1): 10–19, 2020. doi: 10.28991/HEF-2020-01-01-02.

Y. Keskin and G. Oturanc. Reduced differential transform method for generalized kdv equations. *Mathematical and Computational applications*, 15(3):382–393, 2010. doi: 10.3390/mca15030382.

K. S. Kim and S. C. Chapra. Temperature model for highly transient shallow streams. *Journal of Hydraulic Engineering*, 123(1):30–40, 1997. doi: 10.1061/(ASCE)0733-9429(1997)123:1(30).

R. L. Knight, V. W. Payne Jr, R. E. Borer, R. A. Clarke Jr, and J. H. Pries. Constructed wetlands for livestock wastewater management. *Ecological engineering*, 15(1-2):41–55, 2000. doi: 10.1016/S0925-8574(99)00034-8.

J. Li, B. Zhang, M. Liu, and Y. Wang. Numerical simulation of the large-scale malignant environmental pollution incident. *Process Safety and Environmental Protection*, 87(4):232–244, 2009. doi: 10.1016/j.psep.2009.03.001.

N. Meszaros, B. Subedi, T. Stamets, and N. Shifa. Assessment of surface water contamination from coalbed methane fracturing-derived volatile contaminants in sullivan county, indiana, usa. *Bulletin of Environmental Contamination and Toxicology*, 99(3):385–390, 2017. doi: 10.1007/s00128-017-2139-x.

S. R. Moosavi Noori and N. Taghizadeh. Study of convergence of reduced differential transform method for different classes of differential equations. *International Journal of Differential Equations*, 2021, 2021. doi: 10.1155/2021/6696414.

S. Nomura, Y. Ito, S. Takegami, and T. Kitade. Development and validation of an assay method for benzene in the delgocitinib drug substance using conventional hplc. *Chemical Papers*, 73(3):673–681, 2019. doi: 10.1007/s11696-018-0608-2.

B. Noye and H. Tan. Finite difference methods for solving the two-dimensional advection–diffusion equation. *International Journal for Numerical Methods in Fluids*, 9(1):75–98, 1989. doi: 10.1002/fld.1650090107.

E. Permanoon, M. Mazaheri, and S. Amiri. An analytical solution for the advection-dispersion equation inversely in time for pollution source identification. *Physics and Chemistry of the Earth, Parts A/B/C*, 128:103255, 2022. doi: 10.1016/j.pce.2022.103255.

R. K. Saeed and A. A. Mustafa. Numerical solution of fisher–kpp equation by using reduced differential transform method. In *AIP Conference Proceedings*, volume 1888, page 020045. AIP Publishing LLC, 2017. doi: 10.1063/1.5004322.

H. Shi, J. Chen, S. Liu, and B. Sivakumar. The role of large dams in promoting economic development under the pressure of population growth. *Sustainability*, 11(10):2965, 2019. doi: 10.3390/su11102965.

V. K. Srivastava, M. K. Awasthi, and S. Kumar. Analytical approximations of two and three dimensional time-fractional telegraphic equation by reduced differential transform method. *Egyptian Journal of Basic and Applied Sciences*, 1(1): 60–66, 2014. doi: 10.1016/j.ejbas.2014.01.002.

H. W. Streeter. Studies of the pollution and natural purification of the ohio river, part iii, factors concerned in the phenomena of oxidation and reareation. *Public health bulletin*, (146), 1925. URL `http://udspace.udel.edu/handle/19716/1590`.

G. Tchobanoglous, F. L. Burton, and H. D. Stensel. Wastewater engineering. *Management*, 7(1):4, 1991.

M. Tsuji, T. Kawahara, K. Uto, N. Kamo, M. Miyano, J.-i. Hayashi, and T. Tsuji. Efficient removal of benzene in air at atmospheric pressure using a side-on type 172 nm xe2 excimer lamp. *Environmental Science and Pollution Research*, 25 (19):18980–18989, 2018. doi: 10.1007/s11356-018-2103-2.